Annals of Biomedical Engineering, Vol. 27, pp. 617–626, 1999
Printed in the USA. All rights reserved.

0090-6964/99/27(5)/617/10/$15.00

Three-Dimensional Activation Mapping in Ventricular Muscle: Interpolation and Approximation of Activation Times

QUAN NI, ROBERT S. MACLEOD, and ROBERT L. LUX

Nora Eccles Harrison Cardiovascular Research and Training Institute, University of Utah, Salt Lake City, UT

(Received 14 April 1999; accepted 4 June 1999)

Abstract—Interpolation plays an important role in analyzing or visualizing any scalar field because it provides a means to estimate field values between measured sites. A specific example is the measurement of the electrical activity of the heart, either on its surface or within the muscle, a technique known as cardiac mapping, which is widely used in research. While three-dimensional measurement of cardiac fields by means of multielectrode needles is relatively common, the interpolation methods used to analyze these measurements have rarely been studied systematically. The present study addressed this need by applying three trivariate techniques to cardiac mapping and evaluating their accuracy in estimating activation times at unmeasured locations. The techniques were tetrahedron-based linear interpolation, Hardy's interpolation, and least-square quadratic approximation. The test conditions included activation times from both high-resolution simulations and measurements from canine experiments. All three techniques performed satisfactorily at measurement spacing $\leqslant 2$ mm. At the larger interelectrode spacings typical in cardiac mapping (1 cm), Hardy's interpolation proved superior both in terms of statistical measures and qualitative reconstruction of field details. This paper provides extensive comparisons among the methods and descriptions of expected errors for each method at a variety of sampling intervals and conditions. © *1999 Biomedical Engineering Society.* [S0090-6964(99)01105-4]

Keywords—Activation, Cardiac mapping, Interpolation.

INTRODUCTION

A major goal in cardiac electrophysiology is the complete characterization of the spread of activation throughout the heart. One can picture activation as a thin wave front, or set of multiple wave fronts, that moves through the heart along pathways that are dictated by membrane kinetics, cell-to-cell coupling, fiber architecture, and the three-dimensional shape of the heart itself. Detecting the spread of activation on the epicardial and endocardial surfaces of the heart is possible from measurements of electric potential, however, it provides only an incomplete reflection of the underlying behavior. For example, surface-based measurements are often unable to reveal intramyocardial events such as reentrant pathways responsible for cardiac arrhythmias.[25] Hence, to capture cardiac activation completely, it is necessary to record potentials also from within the heart tissue. Multielectrode intramural needles permit such measurements and form the basis of many studies into the fundamental nature of normal and abnormal activation. In recent years, three-dimensional activation mapping has provided detailed information on the roles of anatomical structure in normal activation,[30] on the spatial nature of extracellular stimulation of cardiac tissue,[17] and on some electrophysiological mechanisms of arrhythmias.[13,24]

Recording electric potentials from multiple sites in the heart is known as cardiac mapping, a discrete measuring scheme that reveals both temporal and spatial information. As with any discrete sampling technique, an important question for cardiac mapping is how to determine values at locations from which direct measurements are not available.[21] Interpolation and approximation are the most common approaches for providing values at unmeasured sites but studies of these methods in cardiac mapping are relatively sparse in the literature[5,9,21,22] and have all been limited to epicardial measurements. Our own studies have recently shown that although linear methods of interpolation are very common and simple to implement, they do not perform as well as other slightly more elaborate techniques.[22] The study of three-dimensional cardiac mapping is similarly incomplete in that linear methods are the standard even though they have the same (or worse) shortcomings in three dimensions as they do in surface recordings.

The purpose of this study was to evaluate the accuracy of a selection of interpolation and approximation methods in three-dimensional cardiac activation mapping.[28] We examined these techniques with activation times, which are not directly measurable, but can be derived from measured potential signals. Activation times indicate the time of passage of the activation wave front and characterize the sequence of events during the spread of excitation in the heart. There is a general consensus that no single method can effectively interpo-

Address correspondence to Robert S. MacLeod, Nora Eccles Harrison CVRTI, Building 500, University of Utah, Salt Lake City, UT. Electronic mail: macleod@cvrti.utah.edu

late all physical quantities.[1] While many of the methods described here have their origins in other areas of science and engineering, wherever possible we have adapted and adjusted them for the specific task of interpolating cardiac activation times. Presented here are results from three different families of techniques: tetrahedron-based linear interpolation, Hardy's interpolation, and least-square quadratic approximation. To provide quantitative validation, we have applied these methods to both high-resolution, simulated activation times from a slab of heart tissue and to measured values from acute canine experiments.

METHODS

Interpolation and Approximation

We begin with a general definition of interpolation and approximation problems and then describe the three different methods evaluated in detail here.

Given activation times t_i each associated with a discrete measurement point in three-dimensional space (x_i, y_i, z_i), $i = 1,\ldots,N$, the *interpolation* problem is to find a function $T(x,y,z)$ such that

$$T(x_i, y_i, z_i) = t_i, \quad i = 1,\ldots,N. \tag{1}$$

A closely related problem is *approximation* in which we relax the requirements such that

$$T(x_i, y_i, z_i) \approx t_i, \quad i = 1,\ldots,N. \tag{2}$$

T is usually sought within the finite-dimensional linear interpolation space, which has the general form of

$$T(x,y,z) = \sum_{i=1}^{M} c_i \phi_i(x,y,z), \tag{3}$$

where ϕ_i, $i = 1,\ldots,M$, is a set of basis functions and the coefficients, c_i, are determined by the interpolation [Eq. (1)] or approximation [Eq. (2)] conditions. The assumption associated with interpolation is that the activation values, t_i, are *exact* and thus we force tight agreement between t_i and $T(x_i, y_i, z_i)$. Approximation, on the other hand, assumes some error in the individual measurements and requires only agreement to a degree determined by the application, the measurements, and the specific method.

One consequence of the infinite variety of spatial distributions that can arise in physical problems is that no set of basis functions can be in any way optimal for all purposes. There is no completely satisfactory ''general purpose'' interpolation method, especially for three-dimensional (trivariate) distributions.[1] Furthermore, there are no completely satisfactory closed-form methods known to us with which to select or even optimize the choice of interpolation scheme. Instead, selection and evaluation must rely on empirical criteria, based on samples of the data to be interpolated.

With basis functions and weights determined, $T(x,y,z)$ gives a complete description of the underlying spatial distribution, which can be used to estimate the value at any unsampled observation site (x_p, y_p, z_p) using equation

$$\tilde{t}_p = T(x_p, y_p, z_p) \approx \sum_{i=1}^{M} c_i \phi_i(x_p, y_p, z_p), \tag{4}$$

where M depends on the interpolation/approximation method.

Interpolation and approximation methods can be further differentiated by their scope. In a global method, $T(x,y,z)$ depends on all measurement points regardless of their distance from the observation point **p** (bold notation indicates a vector when lower case and a matrix in upper case throughout the manuscript), whereas a local method uses only measurement points nearby **p** (where the definition of ''nearby'' is part of the specific interpolation or approximation technique). In the case of large sets of data or distributions that change rapidly in space, local schemes often lead to better results at lower computational costs and are more stable numerically.[12,16]

Tetrahedron-Based Linear Interpolation. Tetrahedron-based interpolation is a local technique. It typically involves the following two steps: (1) building a topological structure given regularly or irregularly scattered sample locations, e.g., create a mesh of tetrahedra that connects all measurement points by means of some three-dimensional triangulation scheme; and (2) defining a piecewise polynomial from data values over each element of the mesh, in our case, each tetrahedron. We used Delaunay triangulation, which maximizes the minimum angle of each element.

It is both natural and computationally advantageous to represent a local interpolation scheme in a local coordinate system, such as the Barycentric system, which represents any point **p** with respect to a tetrahedron with vertices $\mathbf{v}_i$, $i = 1,\ldots,4$, in terms of the coordinates b_i, $i = 1,...,4$, as

$$\mathbf{p} = b_1\mathbf{v}_1 + b_2\mathbf{v}_2 + b_3\mathbf{v}_3 + b_4\mathbf{v}_4, \tag{5}$$

with the requirement of normalization

$$b_1 + b_2 + b_3 + b_4 = 1. \tag{6}$$

To determine the coordinates b_i, $i=1,\ldots,4$, for the point (x_p,y_p,z_p), given the tetrahedron (x_i,y_i,z_i), $i=1,\ldots,4$, it is necessary to solve the system

$$\begin{pmatrix} x_1 & x_2 & x_3 & x_4 \\ y_1 & y_2 & y_3 & y_4 \\ z_1 & z_2 & z_3 & z_4 \\ 1 & 1 & 1 & 1 \end{pmatrix} \begin{pmatrix} b_1 \\ b_2 \\ b_3 \\ b_4 \end{pmatrix} = \begin{pmatrix} x_p \\ y_p \\ z_p \\ 1 \end{pmatrix}. \tag{7}$$

The advantage of such a system is that to perform a linear interpolation of the value at a point **p** only requires an inner product of the Barycentric coordinates vector and the values at the vertices of the tetrahedron which contains **p**,

$$T(\mathbf{b})=\mathbf{b}\cdot\mathbf{t}=\sum_{i=1}^{4} b_i t_i. \tag{8}$$

Hardy's Interpolation. A family of basis functions, referred to as radial functions, have achieved great success for providing effective interpolations in various numerical experiments on scattered two-dimensional data.[16,20] These functions depend only on Euclidean distance from the observation point and extend naturally to three dimensions. One of the simplest and most effective radial basis functions used in interpolation is the multiquadric, first developed by Hardy,[19] which has the form

$$T(\mathbf{p})=\sum_{i=1}^{N} c_i\sqrt{\|\mathbf{p}-\mathbf{p}_i\|^2+R^2}, \tag{9}$$

where $\mathbf{p}=(x,y,z)$, $\|\mathbf{p}-\mathbf{p}_i\|^2=(x-x_i)^2+(y-y_i)^2+(z-z_i)^2$, and R^2 is a parameter that must be set based on the particular application.

The coefficients c_i in Eq. (9) are determined by the interpolation conditions [Eq. (1)]. The resulting $N\times N$ linear system is nonsingular,[12] but it becomes ''numerically singular'' as the number of points increases above 100. Even if the system remained nonsingular, the computational overhead of solving large systems makes the global implementation of Hardy's interpolation costly to use in practice. An alternative is to partition the measurement point domain into subdomains such that interpolants are constructed locally on each subdomain. We evaluated different local Hardy's schemes using the simulation datasets which contained over 90,000 points. Our preliminary tests showed that in the range of 10–100 neighbors, mean interpolation errors were stable whereas maximum errors were typically lowest when the number of neighbors included was about 60. We used this same number of neighbors to construct a local interpolant T for each observation point in all tests presented in this paper for Hardy's interpolation.

The accuracy of the Hardy's interpolation depends also on the parameter R, whose optimal value is problem dependent and an open research problem.[10] We used an empirical estimate of R provided by Foley[14] that has the following formula:

$$R_{\text{est}}^2=4[(x_{\max}-x_{\min})(y_{\max}-y_{\min})(z_{\max}-z_{\min})]^{2/3}. \tag{10}$$

Least-Square Approximation. The least-square approximation is a commonly used technique in multivariate data analysis.[14] It is especially useful with measured data containing noise because it does not require the exact matching conditions of Eq. (1) and yet offers a relatively simple means of calculating coefficients for a given basis function set. The least-square approach minimizes the sum of the square of errors between given data and the representation from a set of basis functions. In this study, the basis functions were a set of three-dimensional monomials of degree less than 3, which can be expressed as a ten-element vector

$$\mathbf{\Phi}=(x^2,y^2,z^2,xy,xz,yz,x,y,z,1). \tag{11}$$

We then found the coefficients c_j, $j=1,\ldots,10$, by minimizing the error

$$\sum_{i=1}^{N}\left(\sum_{j=1}^{10} c_j\phi_j-t_i\right)^2. \tag{12}$$

Just as with Hardy's interpolation, least-square approximation can operate both globally and also as a local scheme, a process usually referred to as moving least square. The quantity to minimize then depends on the values only at neighboring nodes, each weighted by its distance from the observation point. Equation (12) becomes

$$\sum_{i=1}^{N_e}\left(\sum_{j=1}^{10} c_j\phi_j-t_i\right)^2 w_i, \tag{13}$$

where N_e is the number of neighboring points and w_i, $i=1,\ldots,N_e$, are weighting coefficients. Typically, $N_e \ll N$. We tested the effect of varying N_e in the range of 15–80, and settled on a value of $N_e=25$, which normally gave the best overall accuracy for the data described in this report.

The resulting system forms a matrix equation

$$\mathbf{Ac}=\mathbf{b}, \tag{14}$$

TABLE 1. Mean/maximum differences (ms) between measured and interpolated simulated data using the three interpolation and approximation techniques. Electrode intervals are the distances between adjacent electrodes in the *x*, *y*, and *z* direction. Exp ID represents different activation sequences, e.g., epi-pn/epi: pacing at the epicardium with/without Purkinje network.

Electrode interval (mm)	Method	Exp ID					
		epi	epi-pn	mid	mid-pn	endo	endo-pn
2-2-1	Linear	0.06/3.04	0.09/3.04	0.07/3.08	0.11/3.08	0.06/2.99	0.11/3.06
	Hardy	0.11/1.35	0.12/1.74*	0.11/1.21	0.11/1.49*	0.11/1.25	0.10/2.29*
	Least square	0.05/2.31	0.11/2.92	0.07/2.30	0.17/2.78	0.06/2.36	0.13/2.78
2-2-2	Linear	0.15/3.22	0.20/4.00	0.18/3.70	0.23/3.84	0.15/3.11	0.17/3.06
	Hardy	0.08/1.52	0.11/2.00	0.08/1.27	0.14/1.94	0.08/1.47	0.09/2.72
	Least square	0.11/3.10	0.19/3.35	0.14/3.01	0.29/3.39	0.11/3.11	0.22/3.15
4-4-2	Linear	0.24/4.70	0.34/5.20	0.28/5.47	0.44/5.47	0.24/4.09	0.40/5.32
	Hardy	0.14/2.33	0.21/5.45	0.14/2.43	0.28/5.47	0.14/1.85	0.29/5.44
	Least square	0.31/5.13	0.50/6.76	0.43/5.24	0.73/6.68	0.30/5.31	0.56/6.10
8-8-2	Linear	0.60/8.07	0.81/9.91	0.65/7.73	1.05/10.94	0.61/7.2	1.02/10.96
	Hardy	0.29/4.58	0.53/9.15	0.33/4.34	0.85/12.05	0.29/4.24	0.94/13.18
	Least square	0.70/8.18	1.02/11.03	0.87/8.51	1.33/11.11	0.70/8.54	1.12/10.66
8-8-5	Linear	1.10/6.94	1.30/9.91	1.33/8.90	1.54/10.94	1.15/7.25	1.25/10.96
	Hardy	0.53/5.13	0.88/8.98	0.76/4.36	1.22/11.69	0.51/4.54	1.07/13.74
	Least square	1.30/12.47	1.62/12.57	1.56/12.14	1.88/13.24	1.29/12.92	1.39/10.74
16-16-5	Linear	2.29/10.13	2.37/13.51*	2.45/15.17	2.43/15.88*	2.32/13.08	1.87/15.88
	Hardy	1.23/11.36	1.69/10.99	1.44/8.78	1.94/13.90	1.01/9.95	1.56/14.43
	Least square	3.68/21.25	4.09/22.06	4.09/19.67	4.03/19.84	3.85/21.35	2.60/15.32

*p=NS for epi vs epi-pn, mid vs mid-pn, and endo vs endo-pn; all others $p<0.0001$.

where the elements of $\mathbf{A}$ are $a(i,j)=\Sigma_{k=1}^{N_e} w(\mathbf{p}_k)\cdot\phi_i(\mathbf{p}_k)\phi_j(\mathbf{p}_k)$ and $b_i=\Sigma_{k=1}^{N_e} w(\mathbf{p}_k)\phi_i(\mathbf{p}_k)t_i$. A frequently used weighting function[14] is

$$w(\mathbf{p}_i)=(1-d_i/d_{\max})^2+0.125, \tag{15}$$

where $d_i=\|\mathbf{p}-\mathbf{p}_i\|$, and $d_{\max}=\max(d_1,...,d_{N_e})$.

Direct methods for solving Eq. (14) are susceptible to roundoff error.[26] One remedy is to use the QR decomposition of $\mathbf{A}$ to express $\mathbf{A}$ as $\mathbf{A}=\mathbf{QR}$, in which $\mathbf{Q}$ is an orthogonal matrix and $\mathbf{R}$ is a triangular matrix. The equation for finding $\mathbf{c}$ then becomes the more numerically stable

$$\mathbf{Rc}=\mathbf{Q}^T\mathbf{b}. \tag{16}$$

Experimental Methods

Just as there is no *a priori* method of selecting the best interpolation method for a particular situation, there is no single best means of testing the performance of interpolation methods. Typical approaches include defining subjectively appropriate analytical test functions or simulating a test dataset. We have taken the latter approach by applying all methods to simulated activation time data provided by Colli Franzone *et al.* Although simulated data offer many advantages with regard to spatial resolution and control over simulation parameters, they do not perfectly represent the reality of measured values. Hence, we also applied all methods to measured activation times from experiments using needle electrodes in the canine ventricle, as described below. In both cases, the test paradigm was similar. From full-resolution simulations or measurements, we selected subsets of points, interpolated back to the full-resolution data, and compared the results.

Simulation Data. The source of the simulated activation time data was an eikonal model of spread of excitation based on an anisotropically conducting parallelepipedal slab consisting of $66\times66\times21$ nodes for a $65\times65\times10$ mm region.[11] Stimulations initiated excitation from points at the epicardium (epi), midwall (mid), and endocardium (endo) along a line perpendicular to the epicardial surface. An additional feature of the model was the optional inclusion of an idealized Purkinje conduction network lining the endocardial surface, thus producing multiple initiation sites of activation for three of the total of six simulation datasets.

In testing the three interpolation methods described above with each of the six simulation datasets, we changed the subsampling resolution applied to define measurement points from 2 to 16 mm in the x and y directions and from 1 to 5 mm in the z direction (see

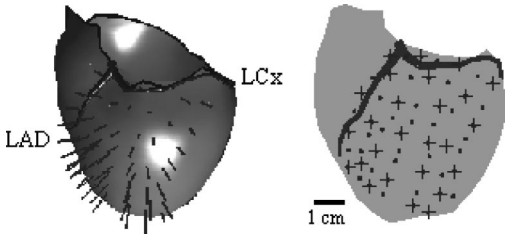

FIGURE 1. Multielectrode needle configuration. Left panel shows positions of multielectrode needles in the left ventricular free wall. LAD refers to left anterior descending coronary artery, and LCx refers to left circumflex coronary artery. Right panel shows the electrode configuration on the epicardium. Crosses mark electrodes selected as measurement points to construct interpolants.

Table 1 for details). Interpolants constructed from the subsampled measurement points provided estimates at all remaining locations in the 90,000 node slab. Interpolation accuracy was evaluated by comparing interpolated values with original values from the simulation.

Experimental Data. The experimental activation times were measured from an isolated perfused canine heart.[31] In the experiment, 56 needles, each with 10 electrodes, were inserted into the free wall of the left ventricle. The average distance between needles was 7.7 ± 1.9 mm on the epicardial surface and 5.4 ± 1.6 mm on the endocardial surface. The distance between electrodes along each needle was 1.6 mm. To construct interpolants, we selected three electrodes (Nos. 1, 5, and 10, placed in the endocardium, midwall, and epicardium, respectively) from 27 of the 56 needles as measurement points. The average distance between the subset of measurement points was 10.3 ± 5.4 mm. Activation times at electrodes not in contact with the myocardium were excluded from the dataset. See Fig. 1 for needle configurations and selected measurement needles.

We sampled unipolar electrograms at 1000 Hz from all channels. The activation time for each electrode site was the time of occurrence of the minimum time derivative in the relevant electrogram. The test data consisted of activation sequences from supraventricular pacing and pacing at epicardial, midwall, and endocardial sites in the left ventricle.

Statistical Analysis

Interpolation and approximation accuracy were described by mean and maximum values of the absolute differences between original values from simulated or measured data and the corresponding values by interpolation. We used the Wilcoxon rank–sum test to perform pairwise comparisons and a Kruskal–Wallis test for comparisons among more than two samples. The null hypothesis was rejected at a significance level of 0.05 ($\alpha = 0.05$).

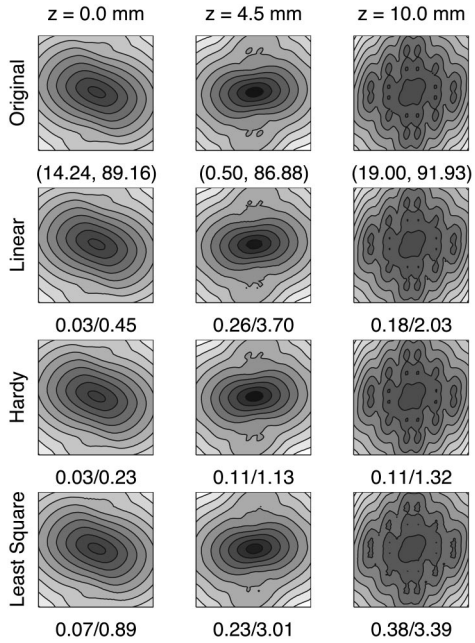

FIGURE 2. Example of interpolation and approximation results with internodal point interval 2-2-2 mm. Stimulation was applied intramurally with the Purkinje network (mid-pn). From left to right are cross sections (65×65 mm^2) at one of three depths ($z = 0$, 4.5, and 10 mm as marked on the top row) from the epicardial surface. Labels under each row indicate mean/max interpolation error of the slice except for labels under the first row of the panel, which show the earliest and latest activation times. There is an 8 ms interval between adjacent contour lines, which are generated using linear interpolation. Dark shading indicates early activation and light shading indicates late activation.

RESULTS

Interpolation of Simulation Data

Table 1 contains a summary of statistical results of the three interpolation and approximation techniques on six simulated activation sequences with progressively coarser subsampling. See Figs. 2 and 3 for isochrone maps from examples of the above tests.

Tetrahedron-Based Linear Interpolation. For linear interpolation, mean errors were negligible (less than 1 ms, which was the sampling resolution of acquisition) for all pacing sequences as long as node spacings were less than 2 mm; maximum errors ranged from 3 to 4 ms. Both mean and maximum errors increased gradually with coarser subsampling, reaching 2 and 10 ms, respectively, for node spacing parallel to the epicardium of 16 mm.

Figure 2 contains an example of a simulated midmyocardially paced beat with 2 mm spacing and the Purkinje

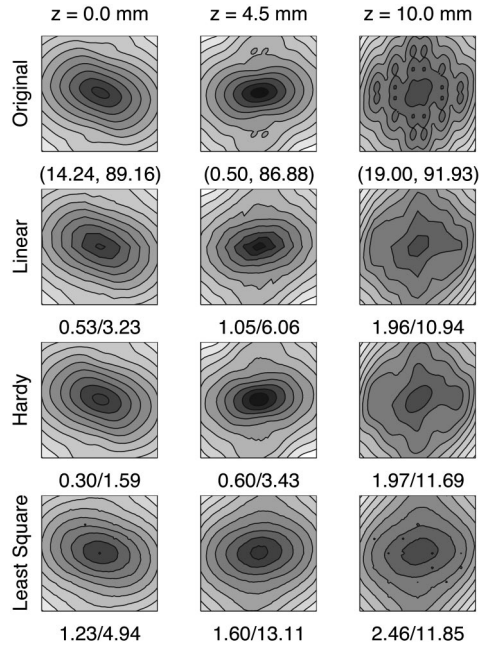

FIGURE 3. Example of interpolation and approximation results for the nodal point intervals of 8-8-5 mm. Same configuration as Fig. 2.

system included. The interpolated activation maps preserve the rotating elliptical shape of the activation front, as well as the discrete features that arise because of the Purkinje system at the subendocardium. When the spacing between nodes in the x and y directions increased to 8 mm and in the z direction to 5 mm, as shown in Fig. 3, interpolated maps still showed the general features of anisotropic propagation. However, local details were lost in the reconstruction such as the extrema at the Purkinje ventricular junctions on the endocardial surface, where interpolation produced the largest mean/maximum error.

The effect of changing pacing locations on interpolation results was minimal. Both mean and maximum absolute errors were similar for epicardial, intramural, and endocardial pacing. The presence of the Purkinje network (PN), however, increased interpolation error significantly ($p<0.0001$ in comparisons between epi versus epi-pn, mid versus mid-pn, and endo versus endo-pn using a Wilcoxon rank–sum test), except for some cases in which subsampling was coarse, e.g., with electrode intervals of 16-16-5 mm, average interpolation error exceeded 2 ms for all but one pacing site. With Purkinje networks included in the simulations, the interpolation error was noticeably higher at the sites of the Purkinje ventricular junctions included in the simulation, as shown in the rightmost column of Fig. 3.

Hardy's Interpolation. As with linear interpolation, coarser subsampling increased the error in Hardy's interpolation. However, the magnitude of interpolation error was always lower than—often half—that of linear interpolation, as illustrated in Table 1. At 8-8-2 mm subsampling, for example, mean absolute errors ranged from 0.53 to 0.94 ms and from 0.29 to 0.33 ms, with and without the Purkinje network, respectively. Equivalent values for linear interpolation were 0.81–1.05 ms and 0.60–0.65 ms, respectively. The responses of Hardy's interpolation results to pacing site and the presence of the Purkinje system were also very similar to those of linear interpolation, but were consistently more accurate except at 2-2-1 mm subsampling when mean absolute errors were very small (around 0.1 ms) in both interpolation methods.

The activation maps using Hardy's interpolation shown in Figs. 2 and 3 illustrate a similar dependence on subsampling density to that found in the linear interpolation case. A characteristic difference between techniques was that the distributions from Hardy's interpolation were consistently smoother than those from linear interpolation as reflected in the contour lines of the maps in Figs. 2 and 3, a feature which was virtually guaranteed because of the higher-order continuity of the interpolants.

One notable feature of Hardy's interpolation is the ability to adjust the parameter R in Eq. (9). To evaluate the effect of varying R, we computed interpolation errors for values of R ranging from $R_{\text{est}}/10$ to $10\times R_{\text{est}}$, where we used Eq. (10) to compute R_{est}. Within this range, rms error varied less than 5% and R_{est} was generally a good estimate of the value of R for which the local minimum of the rms error occurred.

Least-Square Approximation. Least-square approximation showed the same effect of subsampling resolution on estimation error as seen in the linear and Hardy's methods. At 2 mm subsampling, the least-square technique had similar error magnitudes as linear interpolation. When node spacing exceeded 4 mm parallel to the epicardium, however, the least-square approach had the largest mean/maximum errors among the three techniques evaluated.

The activation maps constructed from the least-square approximation shown in Figs. 2 and 3 support the statistical results. Already at 2 mm resolution, the least-square approach started to lose details of some of the earliest activated Purkinje ventricular junctions as shown in the rightmost column of Fig. 2. When subsampling resolution decreased to 8-8-5 mm (Fig. 3), the least-square reconstruction gave smooth contour maps with the largest mean/maximum errors throughout the simulation domain.

Interpolation of Experimental Data

Table 2 contains statistical results of interpolation and approximation from four different activation sequences:

TABLE 2. Mean/maximum differences (ms) between measured and interpolated experimental data.

Exp. ID	Linear	Hardy	Least square
	mean/max	mean/max	mean/max
atdr	2.31/7.58	2.34/11.69	2.13/7.56
epi	2.70/17.84	2.41/16.39	3.06/18.88
mid	2.47/10.68	2.10/11.10	2.54/13.03
endo	2.89/12.48	2.27/12.98	2.60/13.37

pacing from the atria (atdr), the epicardium (epi), the middle of the heart wall (mid), and the endocardium (endo). The three techniques showed comparable accuracy with mean interpolation error ranging from 2 to 3 ms. Overall, Hardy's interpolation had the smallest mean interpolation errors ($p = 0.0002$, Kruskal–Wallis test). All three techniques yielded considerable maximum errors—on the order of 10 ms—but the locations of maximum error were not consistent.

Figure 4 shows an example of interpolation results when the pacing depth was midway between the epicardium and endocardium. The three surfaces at depths of 1.6, 6.4, and 9.6 mm did not contain any of the measurement points from which we constructed the interpolants. In general, the reconstructed activation maps closely resembled the original measurements. All three interpolation methods precisely reproduced the earliest activated region as well as the anisotropic features of propagation. Linear interpolation had results very similar to those from Hardy's interpolation. The least-square approach produced smooth contour lines but obscured the irregularity of activation visible in the latest activated region in the original measurements.

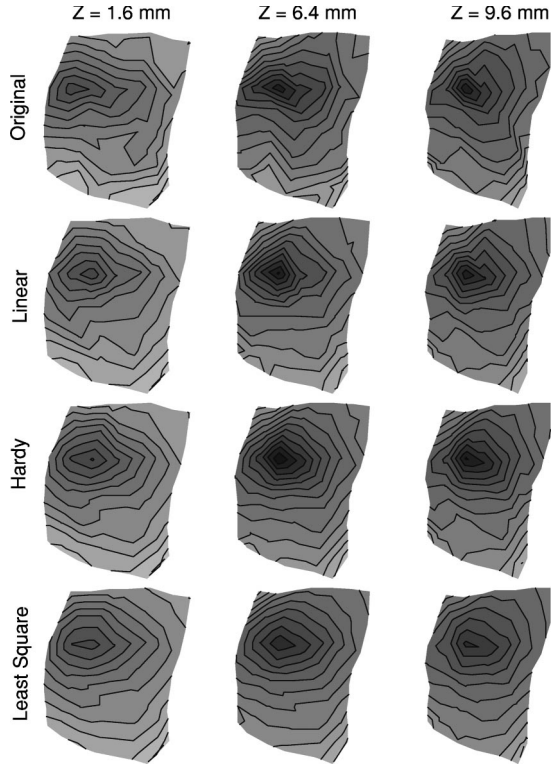

FIGURE 4. Example of interpolation and approximation results from experimental data. Stimulation was applied to the middle of the heart wall (midwall). From left to right are cross sections at one of the three depths ($z = 1.6$, 6.4, and 9.6 mm, from the epicardium). Interval between adjacent contour lines is 4 ms.

Influence of Geometric Errors

All the results presented here were based on the assumption that electrode locations were measured perfectly and did not vary with time. In an experimental setting with a beating heart, the registration error in electrode geometry lies in the range of 2–3 mm for direct digitization and as high as 5 mm if we include heart shape changes between the time of electrical and geometric measurements, which typically occur at the end of the experiment. Because of the delay between electrical activation and contractile response, motion due to contraction during the heart beat does not add to this total error. To assess the influence of geometric measurement error on interpolation, we created a test protocol using the simulated data in which we started with the full slab of tissue with 10-10-5 mm spacing in the x, y, and z directions, respectively, and then added 2.5 mm of random noise to the x direction. For the Hardy and least-square approaches, the interpolation errors increased by about 1 ms in response to this error. The linear method, however, showed mean/maximum error increases from 1.28/4.43 to 7.23/99.93 ms, depending on the pacing protocol.

The relatively high sensitivity of interpolation error to electrode locations in tetrahedral-based methods is especially meaningful when one considers that linear interpolation is the standard approach used by most researchers in cardiac mapping. Morever, linear methods are implicitly part of most computer programs for interpolation and for visualization of three-dimensional scalar fields.

DISCUSSION

Activation mapping is used extensively in clinical settings and experimental investigations to study mechanisms and to guide therapies of arrhythmias. As discussed by Ideker *et al.*,[21] isochronal maps have the following underlying assumptions: (1) acceptable accuracy in geometry and activation registrations and (2) acceptable accuracy in interpolation of any point between measurements. Violations of these assumptions can lead to false interpretation of propagation. This study

sought to address the second assumption and examined interpolation accuracy of a variety of techniques with activation sequences showing different patterns and levels of spatial complexity.

Interpolation Accuracy

Among the three techniques tested in this study, Hardy's interpolation had the best overall accuracy for estimating activation times. This result is consistent with other survey studies that used a variety of test functions and different types of physical data.[16] In our testing with the simulation data, the mean interpolation error for interelectrode spacing of 2 mm was less than 1 ms for all methods. When spacing between subsampled nodes rose to 8 mm, mean interpolation error ranged from 0.3 ms for some cases of Hardy's interpolation to 1.3 ms for least-square approximation. At the same time, the maximum errors were substantially higher, often well above 10 ms for all three methods. At this resolution, none of the methods were capable of capturing the details of activation that were visible on the endocardial surface in simulations that included the Purkinje system. In simulations without the Purkinje system, on the other hand, activation times were captured with good accuracy using Hardy's and linear interpolation methods. It is notable that both the worst (13.18 ms) and the best (4.24 ms) maximum errors for 8 mm spacing arose using Hardy's interpolation and that these results both came from the endocardial pacing site but with and without the Purkinje system, respectively. This finding clearly supports the hypothesis that suitability of an interpolation method depends strongly on the dataset to which it is applied.

Interpolation results based on the measured data from experiments revealed qualitatively similar results. Overall, accuracy was best for Hardy's interpolation but the range of errors was somewhat larger across pacing sites than across interpolation techniques. One result that did not parallel the case of simulated activation times was the dependence of accuracy on activation complexity. In general, atrial pacing is thought to create more numerous, smaller wave fronts and a more complex activation sequence than ectopic pacing from a ventricular site. Our results, however, showed that epicardial pacing resulted in the largest interpolation errors. A more complete test of this hypothesis would be to use electrograms recorded with an intact conduction system and then apply a selective toxin to suppress Purkinje excitability and repeat the measurements.

An important question in cardiac mapping is the minimum spatial sampling rate required to reconstruct the path of activation from discrete measurements. A rigorous theoretical definition of such criteria is obstructed by the lack of adequate metric for information content of the activation and of the relationship between such a metric and spatial sampling density.[22] A more practical approach is to define the minimum spatial sampling rate to be the one that allows the reconstruction of activation times at unmeasured locations with errors that are within the resolution of the measurement system. This study showed that at 2 mm resolution, the interpolation error was less than 1 ms—the theoretical error of 1 ms dictated by the 1000 Hz sampling rates—for all three methods based on the simulated activation times. These results support the findings of a previous experimental study[2] involving high-resolution measurements on the epicardial surface that suggested that a 2 mm sampling rate is adequate to reproduce the path of activation in the heart at least under conditions of normal physiology.

Comparison of Interpolation Methods

We evaluated three types of interpolation and approximation techniques that are commonly used in other engineering fields such as geological survey,[19] computer-aided geometry design,[1] and computer graphics.[23] These techniques are applicable to both two- and three-dimensional datasets and are thus suitable for cardiac mapping, an application in which the locations of the measurements can be irregular and lie on the heart surface as well as within the myocardium.

Tetrahedron-based interpolation is a standard, local technique. It is a natural extension of one-dimensional piecewise polynomial interpolation or two-dimensional triangle-based interpolation into three-dimensional space. A required component of this scheme is a tetrahedral mesh, which for large numbers of irregularly spaced measurements sites can pose a technical challenge and generally yields nonunique meshes. An additional source of ambiguity in generating tetrahedra is the lack of clear dependence between mesh configuration and interpolation accuracy. While the assumptions of Delaunay triangulation are often considered superior for numerical estimation approaches such as the finite-element method, we know of no literature that examines this question in the context of interpolation.

It is possible to extend tetrahedral interpolation methods to higher-order interpolants; however, basis functions with degree higher than 1 require not only data values at the tetrahedron vertices but also spatial derivative information,[15] which is usually unknown from the dataset. Though there are algorithms for derivative generation,[29] these, too, are interpolation or approximation schemes and thus add an unknown source of error to the computation. As a result, in most applications, it is safest to use linear polynomials as the basis function, a practice we followed in this study. Frazier *et al.* used the same approach[18] to determine the potential field based on measurements at multiple locations in the right ventricle. A direct comparison of results obtained from these two

studies is not available due to the difference in interpolating variables, electrical potentials in their study versus activation times in ours.

Hardy's interpolation differs from tetrahedron-based linear methods in terms of basis functions, geometric assumptions, and spatial support. It exists in both global and local implementations. The global form is based on all measured data points, which in practice often leads to solving large and numerically unstable linear systems for each different dataset. Any local form of Hardy's interpolation requires a choice of the number of neighbors used for construction. We found using 60 nearest measurement points kept the size of the linear system within reasonable computational and numerically stable bounds and also suppressed the influence of points that were far away from the observation points.

The least-square approach is fundamentally different from the other two interpolation methods because of the relaxation in the requirement that measured values are considered free of error. It is similar, however, in that the accuracy of least-square approximation depends highly on the match between the basis functions and the underlying field distribution. The rationale for our choice of quadratic polynomial basis functions lay in the ellipsoidal shape of activation wave fronts in the myocardium.[27] Our preliminary unpublished results as well as results from others[4] showed that quadratics performed much better than linear basis functions in approximation but at a substantial cost in computational complexity. A complete set of quadratic basis functions has ten elements [Eq. (11)], which leads to a linear system of coefficients similar to that of a Hilbert matrix. Such systems are known to be sensitive to the contents of the right-hand side of Eq. (14) so that numerical stability becomes a concern.[3] By using the QR decompposion and limiting the number of neighbors to 25, we were able to achieve a consistently reasonable numerical solution.

An important practical consideration in using these interpolation techniques is their relative speed and computational cost. In the tetrahedron-based linear method, the two most costly components are the triangulation process (performed just once for each electrode configuration) and the search for the tetrahedron that contains the observation point (performed repeatedly, once for each selected observation point). The global versions of both the Hardy and least-square approaches require solving a linear system of a size equal to the total number of measurement points. Their local implementations result in systems of potentially much smaller size that have to be recomputed repeatedly for every observation point, a relatively slow process. To provide at least an approximate measure of the total costs involved in each of the three methods described here, we implemented each using MATLAB with no special optimization and observed an approximate ratio of computation times of 9:9:1 for the linear, Hardy's, and least-square methods, respectively. These results did not include the tetrahedralization time and might be expected to change significantly with a more specialized code or computer hardware.

Limitations of the Study

The literature on multivariate interpolation is sparse in cardiac mapping but more prevalent in the broad arena of engineering and numerical mathematics. We have chosen only three representative techniques and tested their utility for estimating activation times in the heart. Our choices were based on recent reviews[1,15] and reported results based on other sources of data.[16] Thus, while this comparative study is by no means exhaustive, it nonetheless reflects a selection based on the salient features of the intended application. In addition, all three techniques evaluated here have some *ad hoc* parameters whose adjustment will affect the accuracy of the results. We have tested a range of candidate values and chosen those which provided acceptable, stable solutions. We note, however, that the optimal values of, for example, R in Hardy's interpolation or the number of neighbors used in the local versions of Hardy's and least-square techniques, remain open research questions.

Our test data included activation sequences from simulations and experimental recordings of normal cardiac tissue. Under pathological conditions, such as ischemia or infarction, abnormal conduction can lead to delay, block, and reentry, which can exhibit more complex activation patterns than under healthy conditions.[6–8] Interpolation errors may change because of the resulting variation in the distribution of activation times; however, our results, based on the experimental data paced at different sites, suggest that additional activation complexity does not always reduce interpolation accuracy. Testing of interpolation during abnormal conduction requires simulations or recordings from hearts under pathophysiological conditions, and this is an ongoing project in our laboratory.

ACKNOWLEDGMENTS

The authors gratefully acknowledge Dr. B. Taccardi of the Cardiovascular Research and Training Institute, Utah for providing the experimental data and Dr. P. Colli Franzone of the University of Pavia, Italy for providing the simulation data used in this study. The support for this work comes from the National Institute of Health under Grant No. HL42388, the Nora Eccles Treadwell Foundation, and the Richard A. and Nora Eccles Harrison Fund for Cardiovascular Research.

REFERENCES

[1] Alfeld, P. In: Mathematical Methods in CAGD, edited by T. Lyche and L. L. Schumaker. New York: Academic, 1989, pp. 1–33.

[2] Arisi, G., E. Macchi, S. Baruffi, S. Spaggiari, and B. Taccardi. Potential fields on the ventricular surface of the exposed dog heart during normal excitation. *Circ. Res.* 52:706–715, 1983.

[3] Atkinson, K. E. An Introduction to Numerical Analysis, 2nd ed. New York: Wiley, 1988.

[4] Barnette, A. R., P. V. Bayly, S. Zhang, G. P. Walcott, R. E. Ideker, and W. M. Smith. Estimation of 3-D conduction velocity fields from cardiac mapping data. *Comput. Cardiol.* 25:605–608, 1998.

[5] Barr, R. C., T. M. Gallie, and M. S. Spach. Automated production of contour maps for electrophysiology. I. Problem definition, solution strategy, and specification of geometric model. *Comput. Biomed. Res.* 13:142–153, 1980.

[6] Bayly, P. V., E. E. Johnson, S. F. Idriss, R. E. Ideker, and W. M. Smith. Efficient electrode spacing for examining spatial organization during ventricular fibrillation. *IEEE Trans. Biomed. Eng.* 40:1060–1066, 1993.

[7] Bayly, P. V., E. E. Johnson, P. D. Wolf, H. S. Greenside, W. M. Smith, and R. E. Ideker. A quantitative measurement of spatial order in ventricular fibrillation. *J. Cardiovasc. Electrophysiol.* 4:533–546, 1993.

[8] Berbari, E. J., P. Lander, B. J. Scherlag, R. Lazzara, and D. B. Geselowitz. Ambiguities of epicardial mapping. *J. Electrocardiol. Suppl.* 24:16–20, 1991.

[9] Blanchard, S. M., R. J. Damiano, W. M. Smith, R. E. Ideker, and J. W. Lowe. Interpolating unipolar epicardial potentials from electrodes separated by increasing distances. *PACE* 12:1938–1955, 1989.

[10] Carlson, R. E., and T. A. Foley. The parameter R^2 in multiquadric interpolation. *Comput. Math. Appl.* 21:29–42, 1991.

[11] Colli Franzone, P., L. Guerri, and B. Taccardi. Spread of excitation in a myocardial volume: Simulation studies in a model of anisotropic ventricular muscle activated by point stimulation. *J. Cardiovasc. Electrophysiol.* 4:144–160, 1993.

[12] Dyn, N. In: Topics in Multivariate Approximation, edited by C. K. Chui, L. L. Schumaker, and F. I. Utreras. New York: 1987, pp. 47–61.

[13] El-Sherif, N., M. Chinushi, E. B. Caref, and M. Restivo. Electrophysiological mechanism of the characteristic electrocardiographics morphology of Torsade de Points tachyarrhythmias in the long-QT syndrome: Detailed analysis of ventricular tridimensional activation patterns. *Circulation* 96:4392–4399, 1997.

[14] Foley, T. A. Interpolation and approximation of 3-D and 4-D scattered data. *Comput. Math. Appl.* 13:711–740, 1987.

[15] Foley, T. A., and H. Hagen. In: Surveys on Mathematics for Industry. Berlin: Springer, 1994, Vol. 4, pp. 71–84.

[16] Franke, R. Scattered data interpolation: Test of some methods. *Math. Comput.* 38:181–200, 1982.

[17] Frazier, D. W., W. Krassowska, P. S. Chen, P. D. Wolf, N. D. Danieley, M. W. Smith, and R. E. Ideker. Transmural activations and stimulus potentials in three-dimensional anisotropic canine myocardium. *Circ. Res.* 63:135–146, 1988.

[18] Frazier, D. W., W. Krassowska, P. S. Chen, P. D. Wolf, E. G. Dixon, M. W. Smith, and R. E. Ideker. Extracellular field required for excitation in three-dimensional anisotropic canine myocardium. *Circ. Res.* 63:147–164, 1988.

[19] Hardy, R. L. Multiquadric equations of topography and other irregular surfaces. *J. Geophys. Res.* 76:1905–1915, 1971.

[20] Hardy, R. L. Theory and applications of the multiquadric-biharmonic method. *Comput. Math. Appl.* 19:163–208, 1990.

[21] Ideker, R. E., W. M. Smith, S. M. Blanchard, S. L. Reiser, E. V. Simpson, P. D. Wolf, and N. D. Danieley. The assumptions of isochronal cardiac mapping. *PACE* 12:456–478, 1989.

[22] Ni, Q., R. S. MacLeod, R. L. Lux, and B. Taccardi. A novel interpolation method for electric potential fields in the heart during excitation. *Ann. Biomed. Eng.* 26:597–607, 1998.

[23] Nielsen, P. M. F., I. J. Le Grice, B. H. Smaill, and P. J. Hunter. Mathematical model of geometry and fibrous structure of the heart. *Am. J. Physiol.* 260:H1365–H1378, 1991.

[24] Pogwizd, S. M., M. Chung, and M. E. Cain. Termination of ventricular tachycardia in the human heart: Insights from three-dimensional mapping of nonsustained and sustained ventricular tachycardias. *Circulation* 95:2528–2540, 1997.

[25] Pogwizd, S. M., and P. B. Corr. Reentrant and nonreentrant mechanisms contribute to arrhythmogenesis during early myocardial ischemia: Results using three-dimensional mapping. *Circ. Res.* 61:352–371:1987.

[26] Press, W. H., S. A. Teukolsky, W. T. Vetterling, and B. P. Flannery, Numerical Recipes in C: The Art of Scientific Computing, 2nd ed. Cambridge: Cambridge University Press, 1992.

[27] Roberts, D. E., L. T. Hersh, and A. M. Scher. Influence of cardiac fiber orientation on wavefront voltage, conduction velocity, and tissue resistivity in the dog. *Circ. Res.* 44:701–712, 1979.

[28] Rogers, J. M., P. V. Baylay, R. E. Ideker, and W. M. Smith. Quantitative techniques for analyzing high-resolution cardiac-mapping data. *IEEE Eng. Med. Biol. Mag.* 17:62–72, 1998.

[29] Stead, S. E.. Estimation of gradients from scattered data. *Rocky Mt. J. Math.* 14:265–279, 1984.

[30] Taccardi, B., R. L. Lux, P. R. Ershler, R. S. MacLeod, T. J. Dustman, and N. Ingebrigtsen. Anatomical architecture and electrical activity of the heart. *Acta Cardiol.* LII:91–105, 1997.

[31] Taccardi, B., E. Macchi, R. L. Lux, P. R. Ershler, S. Spaggiari, S. Baruffi, and Y. Vyhmeister. Effect of myocardial fiber direction on epicardial potentials. *Circulation* 90:3076–3090, 1994.